
Numerical simulations of the collision of an inhomogeneous stellar wind and a relativistic pulsar wind in a binary system

Xavier Paredes-Fortuny

V. Bosch-Ramon, M. Perucho, M. Ribó

High-Energy Phenomena in Relativistic Outflows - V

6 October 2015, La Plata

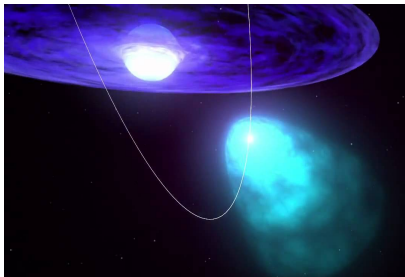
Outline

1. Introduction
2. Clump impact on the colliding wind region
3. Results
4. Discussion
5. Work in progress

1. Introduction
2. Clump impact on the colliding wind region
3. Results
4. Discussion
5. Work in progress

Introduction

We study the interaction of a **relativistic pulsar wind** and an **inhomogeneous stellar wind** in binary systems.



- The collision between the two winds creates a **shock structure**.
- Sources of stellar wind **inhomogeneities**:
 - **Instabilities** in the inner wind (Lucy & Solomon 1970).
 - **Rotation, magnetic fields**, or non-radial pulsations (Cranmer & Owocki 1996).
 - The truncation of the *Be* star equatorial **decretion disk** (Okazaki et al. 2011).
- The presence of **clumps** can **distort** the overall interaction structure (Bosch-Ramon 2013).
- This can affect the **radiative output**.

We perform numerical **Relativistic Hydrodynamical simulations**.

Outline

1. Introduction
2. Clump impact on the colliding wind region
3. Results
4. Discussion
5. Work in progress

Clump impact on the colliding wind region I

The relativistic Euler equations can be written using the **vector of conserved variables**, \mathbf{U} , and the **flux vector**, \mathbf{F} as

$$\mathbf{U}_t + \mathbf{F}^i(\mathbf{U})_{x^i} = 0, \quad i = 1, 2, 3 \quad (1)$$

$$\mathbf{U} = \begin{bmatrix} \rho W \\ \rho h W^2 v^1 \\ \rho h W^2 v^2 \\ \rho h W^2 v^3 \\ \rho h W^2 c^2 - p - \rho W c^2 \end{bmatrix}, \quad \mathbf{F}^1 = \begin{bmatrix} \rho W v^1 \\ \rho h W^2 v^1 v^1 + p \\ \rho h W^2 v^2 v^1 \\ \rho h W^2 v^3 v^1 \\ \rho h W^2 c^2 v^1 - \rho W c^2 v^1 \end{bmatrix}, \quad (2)$$

being the **conserved quantities** and v^i measured in the *laboratory frame*, and the **physical quantities** ρ and p measured in the *local rest frame* (e.g., Martí & Müller 2003).

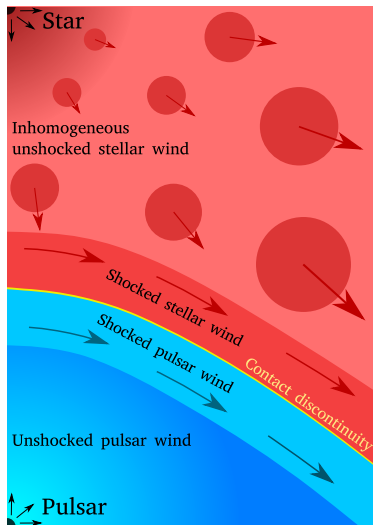
Clump impact on the colliding wind region II

The simulations were performed using a **finite-difference code** based on a high-resolution shock-capturing scheme that solves the multidimensional **equations of RHD in a conservation form** (Martí et al 1997).

- The code is parallelized using **OpenMP** (Perucho et al. 2005).
- The **intercell fluxes** are computed using Marquina's approach (see Donat & Marquina 1996).
- The **intercell physical quantities** are computed with a conservative monotonic parabolic reconstruction of the physical variables (**PPM**; see Woodward & Colella 1984; Martí & Müller 1996; and Mignone et al. 2005).
- The **time integration** is performed using a **Runge-Kutta** formula.

Clump impact on the colliding wind region III

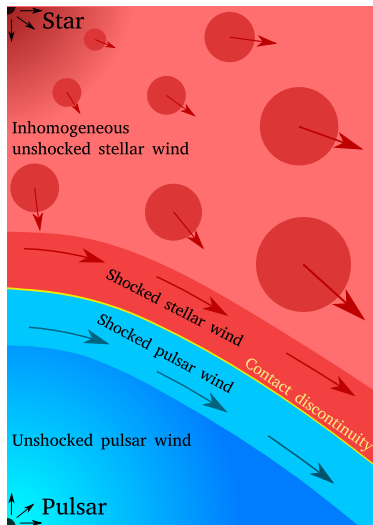
We performed **axisymmetric RHD simulations** of the interaction of a **relativistic pulsar wind** and an **inhomogeneous stellar wind (1 clump)**.



- **Ideal gas** with single particle species and $\hat{\gamma} = 1.444$ (cold protons and relativistic electrons).
- **Grid size:** $l_r = 2.4 \times 10^{12}$ cm, $l_z = 4.0 \times 10^{12}$ cm.
- The adopted **resolution** is 150×250 cells.
- The **star** is located at $(r_0, z_0) = (0, 4.8 \times 10^{12})$ cm.
- The **pulsar** is placed at $(r_0, z_0) = (0, 0.4 \times 10^{12})$ cm.
- The star-pulsar **separation** is of $d_{\text{star-pulsar}} = 4.4 \times 10^{12}$ cm.

Clump impact on the colliding wind region III

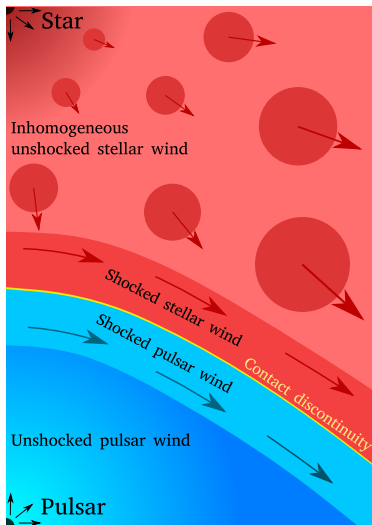
We performed **axisymmetric RHD simulations** of the interaction of a **relativistic pulsar wind** and an **inhomogeneous stellar wind (1 clump)**.



- The lower and right **boundaries** are set to outflow. The left boundary is set to reflection.
- The **stellar wind** is injected as a boundary condition at the top of the grid.
- The **pulsar wind** is injected at a radius of 2.4×10^{11} cm (15 cells).
- The **stellar mass-loss rate** is $\dot{M} = 10^{-7} M_{\odot} \text{ yr}^{-1}$.
- The **pulsar total luminosity** is $L_{\text{sd}} = 10^{37} \text{ erg s}^{-1}$ with Lorentz factor $\Gamma = 6$.
- The pulsar-to-stellar wind **thrust ratio** of $\eta \sim 0.2$.

Clump impact on the colliding wind region III

We performed **axisymmetric RHD simulations** of the interaction of a **relativistic pulsar wind** and an **inhomogeneous stellar wind (1 clump)**.



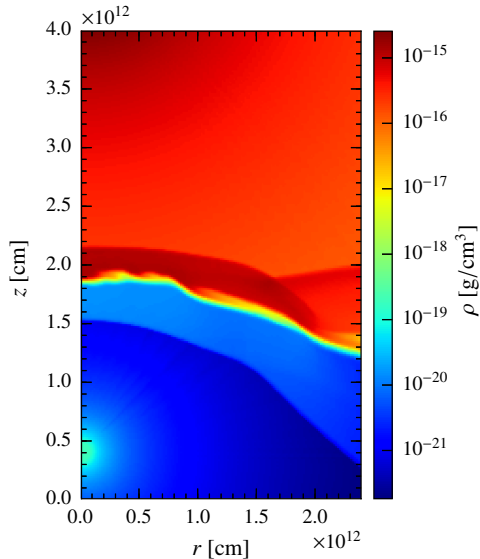
- Set-up of the inhomogeneous stellar wind:
 - ① We obtained a **quasi-steady state** of the two-wind interaction considering an **homogeneous stellar wind**.
 - ② We introduced the stellar wind **inhomogeneity** characterized by a **single clump** centered at the z axis.
- We simulated 4 cases:

χ	R_{clump}	Description
10	$8 \cdot 10^{10}$ cm	light and small
10	$2 \cdot 10^{11}$ cm	light and medium
10	$4 \cdot 10^{11}$ cm	light and large
30	$8 \cdot 10^{10}$ cm	dense and small

Outline

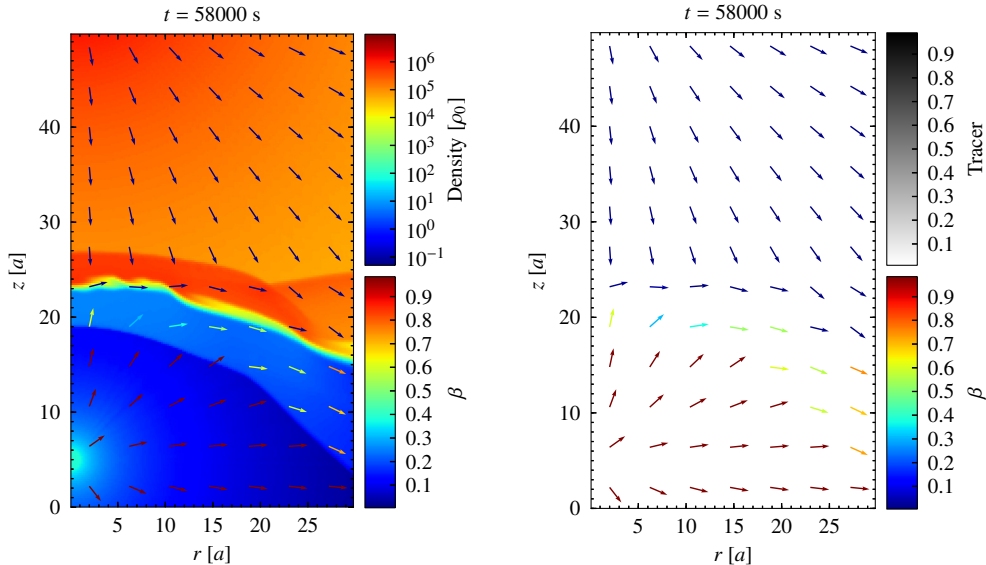
1. Introduction
2. Clump impact on the colliding wind region
- 3. Results**
4. Discussion
5. Work in progress

Results I



The results presented here have already been **published** in X. Paredes-Fortuny, V. Bosch-Ramon, M. Perucho, and M. Ribó (2015)

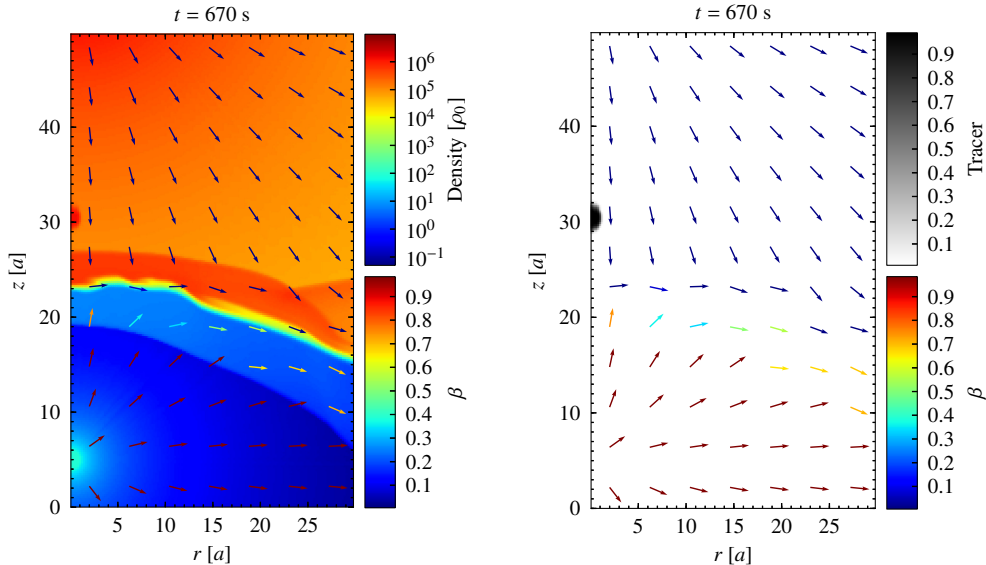
Results II — light and small size clump



Clump: $\chi = 10$, $R_{\text{clump}} = 1 \text{ a} = 8 \cdot 10^{10} \text{ cm}$

Code units: $\rho_0 = 22.5 \times 10^{-22} \text{ g cm}^{-3}$, $a = 8 \times 10^{10} \text{ cm}$ | $d_{\text{star-pulsar}} = 4.4 \times 10^{12} \text{ cm}$.

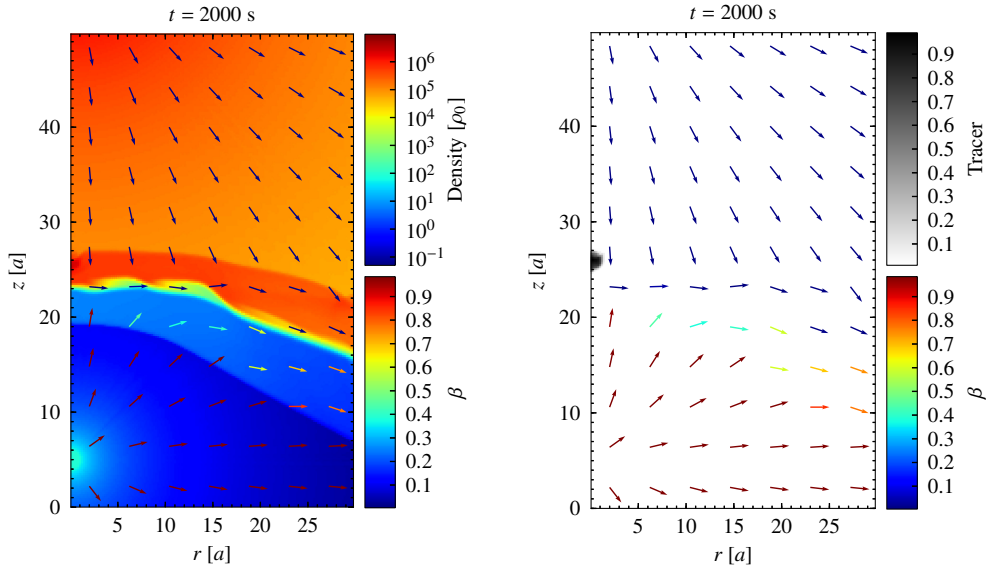
Results II — light and small size clump



Clump: $\chi = 10$, $R_{\text{clump}} = 1 \text{ a} = 8 \cdot 10^{10} \text{ cm}$

Code units: $\rho_0 = 22.5 \times 10^{-22} \text{ g cm}^{-3}$, $a = 8 \times 10^{10} \text{ cm}$ | $d_{\text{star-pulsar}} = 4.4 \times 10^{12} \text{ cm}$.

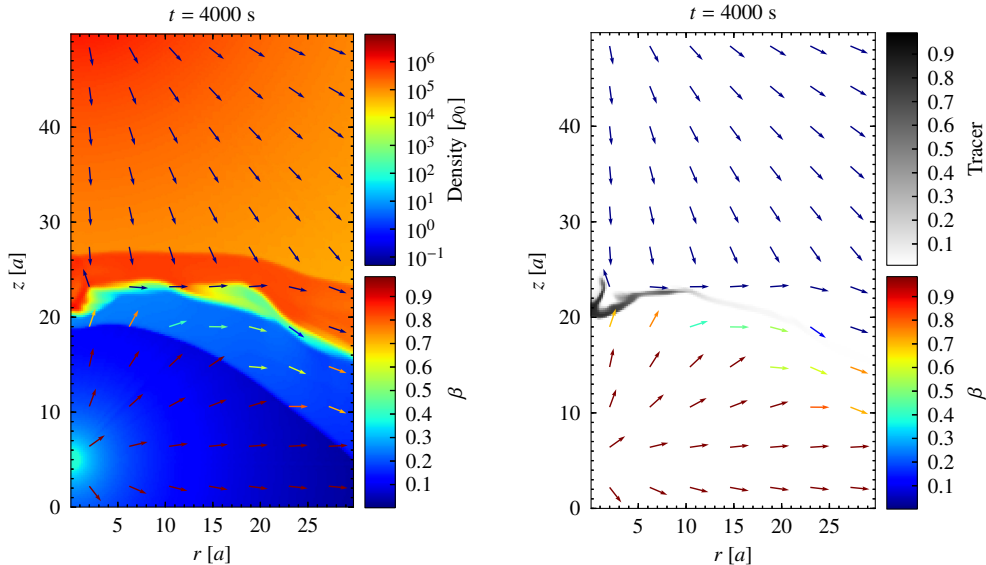
Results II — light and small size clump



Clump: $\chi = 10$, $R_{\text{clump}} = 1 \text{ a} = 8 \cdot 10^{10} \text{ cm}$

Code units: $\rho_0 = 22.5 \times 10^{-22} \text{ g cm}^{-3}$, $a = 8 \times 10^{10} \text{ cm}$ | $d_{\text{star-pulsar}} = 4.4 \times 10^{12} \text{ cm}$.

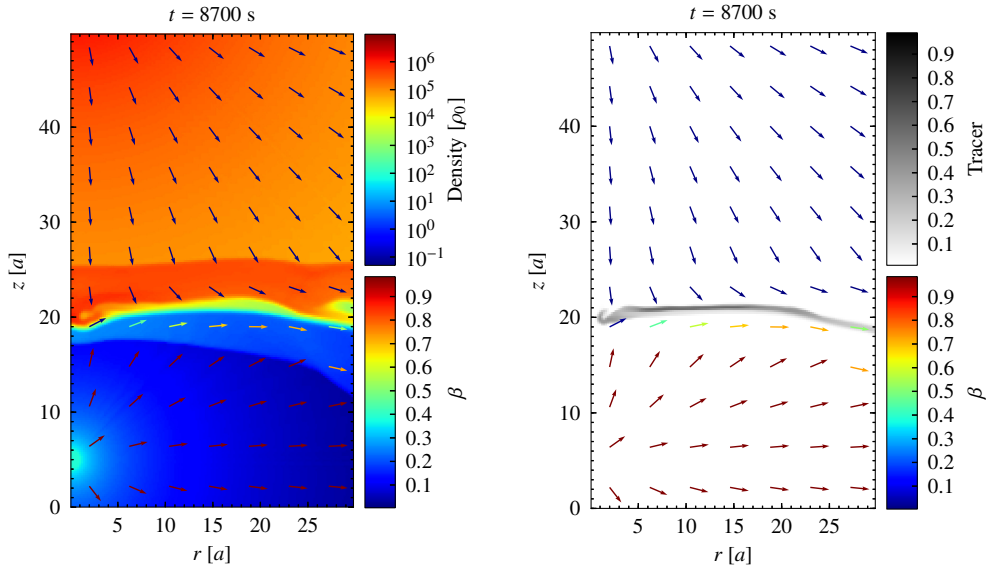
Results II — light and small size clump



Clump: $\chi = 10$, $R_{\text{clump}} = 1 \text{ a} = 8 \cdot 10^{10} \text{ cm}$

Code units: $\rho_0 = 22.5 \times 10^{-22} \text{ g cm}^{-3}$, $a = 8 \times 10^{10} \text{ cm}$ | $d_{\text{star-pulsar}} = 4.4 \times 10^{12} \text{ cm}$.

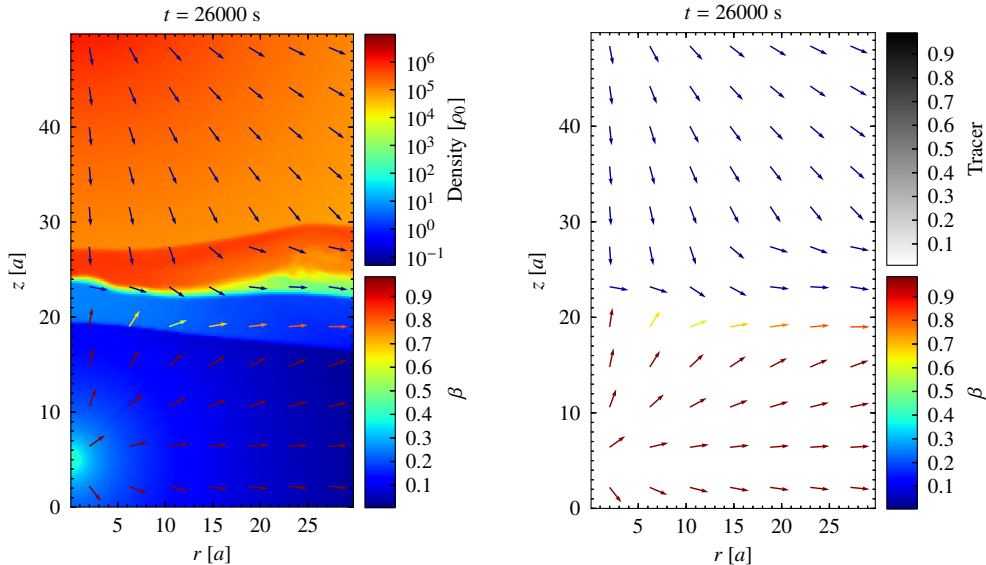
Results II — light and small size clump



Clump: $\chi = 10$, $R_{\text{clump}} = 1 \text{ a} = 8 \cdot 10^{10} \text{ cm}$

Code units: $\rho_0 = 22.5 \times 10^{-22} \text{ g cm}^{-3}$, $a = 8 \times 10^{10} \text{ cm}$ | $d_{\text{star-pulsar}} = 4.4 \times 10^{12} \text{ cm}$.

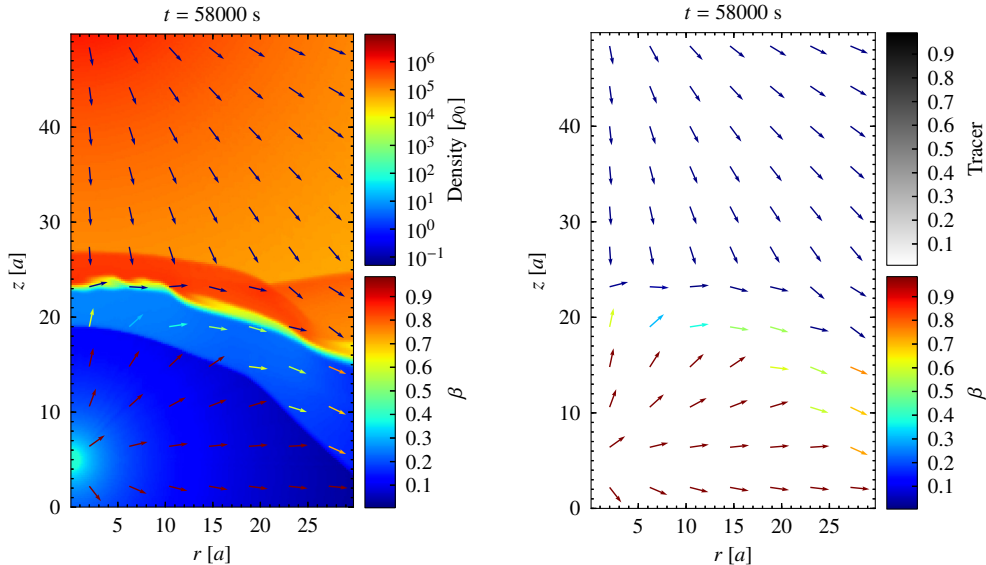
Results II — light and small size clump



Clump: $\chi = 10$, $R_{\text{clump}} = 1 \text{ a} = 8 \cdot 10^{10} \text{ cm}$

Code units: $\rho_0 = 22.5 \times 10^{-22} \text{ g cm}^{-3}$, $a = 8 \times 10^{10} \text{ cm}$ | $d_{\text{star-pulsar}} = 4.4 \times 10^{12} \text{ cm}$.

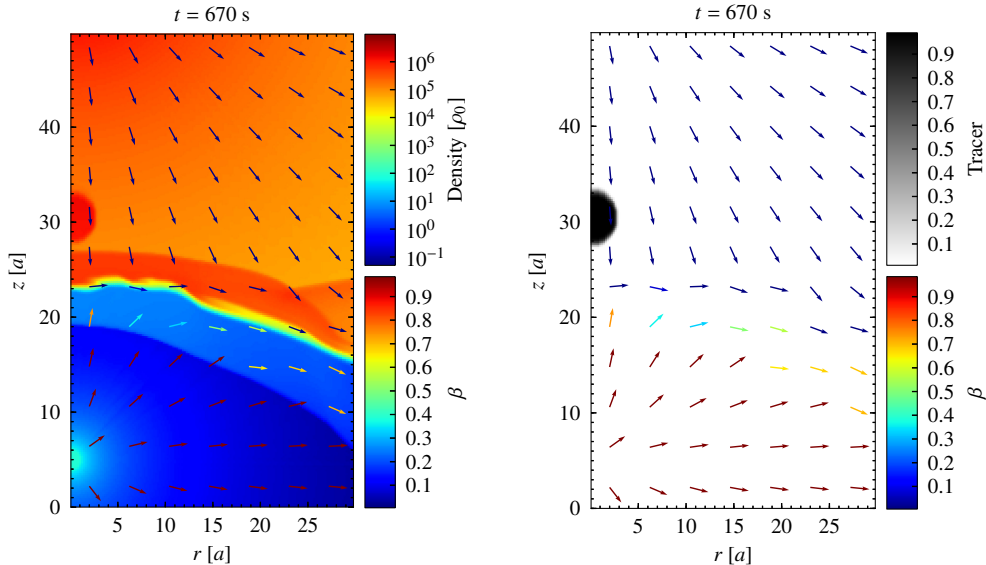
Results III — light and medium size clump



Clump: $\chi = 10$, $R_{\text{clump}} = 2.5 a = 2 \cdot 10^{11}$ cm

Code units: $\rho_0 = 22.5 \times 10^{-22}$ g cm $^{-3}$, $a = 8 \times 10^{10}$ cm | $d_{\text{star-pulsar}} = 4.4 \times 10^{12}$ cm.

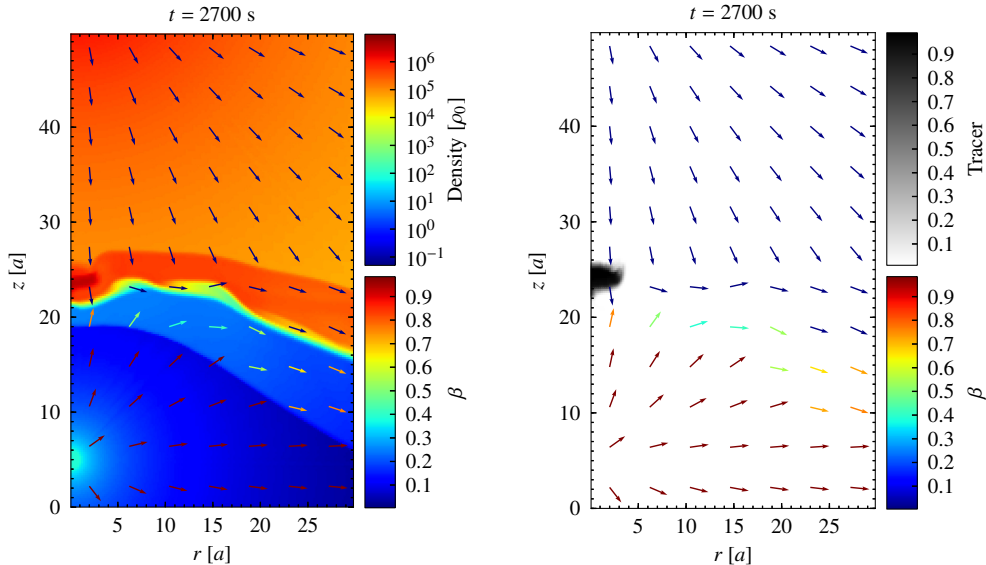
Results III — light and medium size clump



Clump: $\chi = 10$, $R_{\text{clump}} = 2.5 a = 2 \cdot 10^{11} \text{ cm}$

Code units: $\rho_0 = 22.5 \times 10^{-22} \text{ g cm}^{-3}$, $a = 8 \times 10^{10} \text{ cm}$ | $d_{\text{star-pulsar}} = 4.4 \times 10^{12} \text{ cm}$.

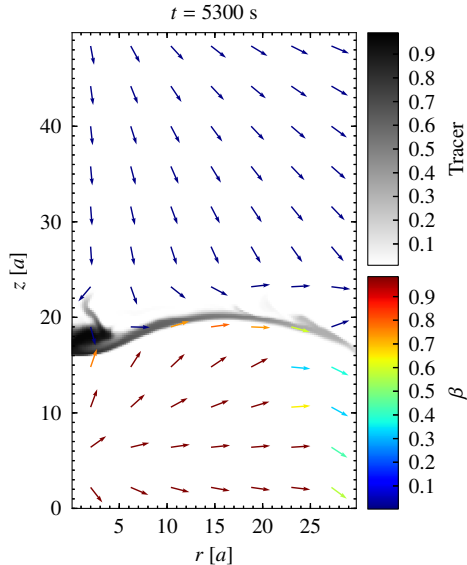
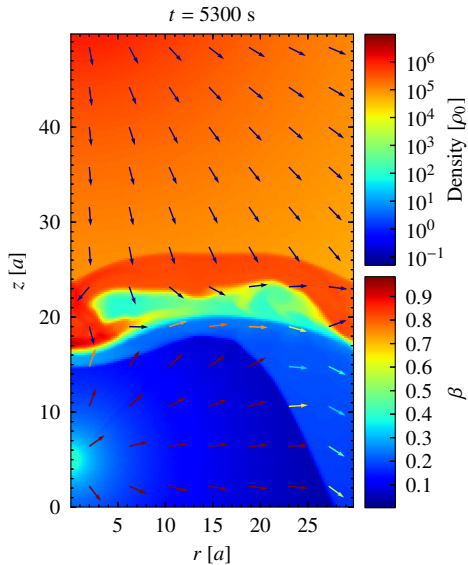
Results III — light and medium size clump



Clump: $\chi = 10$, $R_{\text{clump}} = 2.5 a = 2 \cdot 10^{11}$ cm

Code units: $\rho_0 = 22.5 \times 10^{-22}$ g cm $^{-3}$, $a = 8 \times 10^{10}$ cm | $d_{\text{star-pulsar}} = 4.4 \times 10^{12}$ cm.

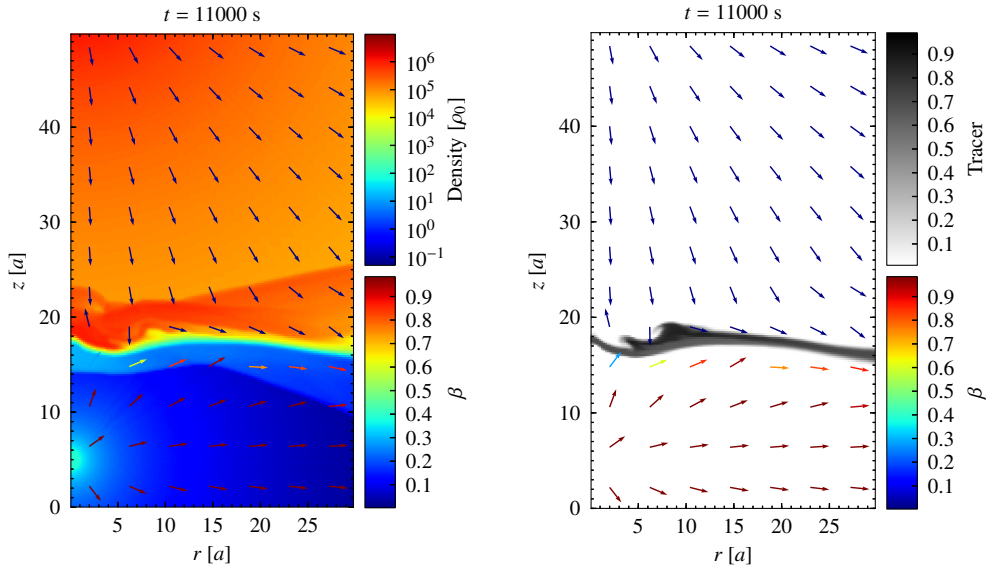
Results III — light and medium size clump



Clump: $\chi = 10$, $R_{\text{clump}} = 2.5 a = 2 \cdot 10^{11}$ cm

Code units: $\rho_0 = 22.5 \times 10^{-22}$ g cm $^{-3}$, $a = 8 \times 10^{10}$ cm | $d_{\text{star-pulsar}} = 4.4 \times 10^{12}$ cm.

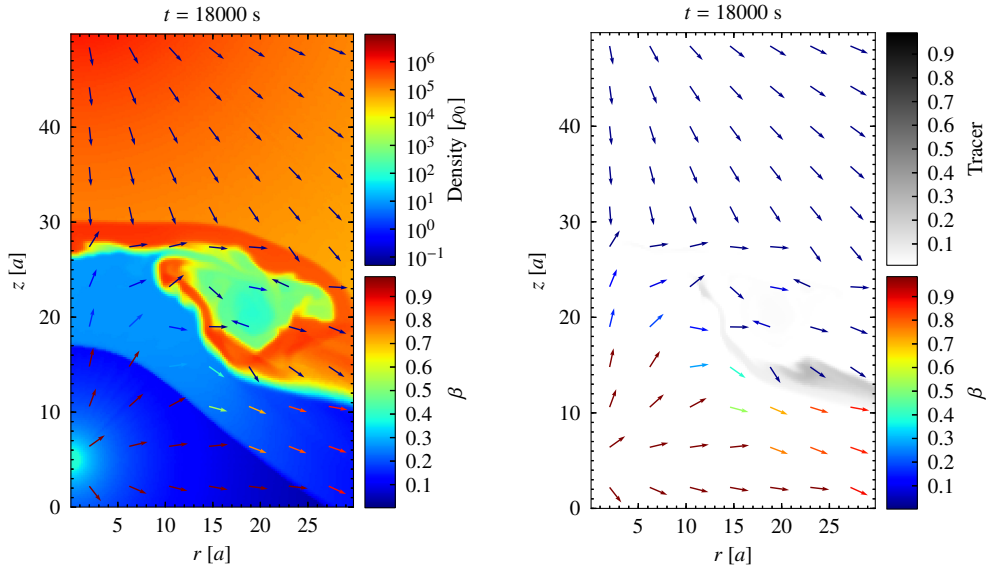
Results III — light and medium size clump



Clump: $\chi = 10$, $R_{\text{clump}} = 2.5 a = 2 \cdot 10^{11}$ cm

Code units: $\rho_0 = 22.5 \times 10^{-22}$ g cm $^{-3}$, $a = 8 \times 10^{10}$ cm | $d_{\text{star-pulsar}} = 4.4 \times 10^{12}$ cm.

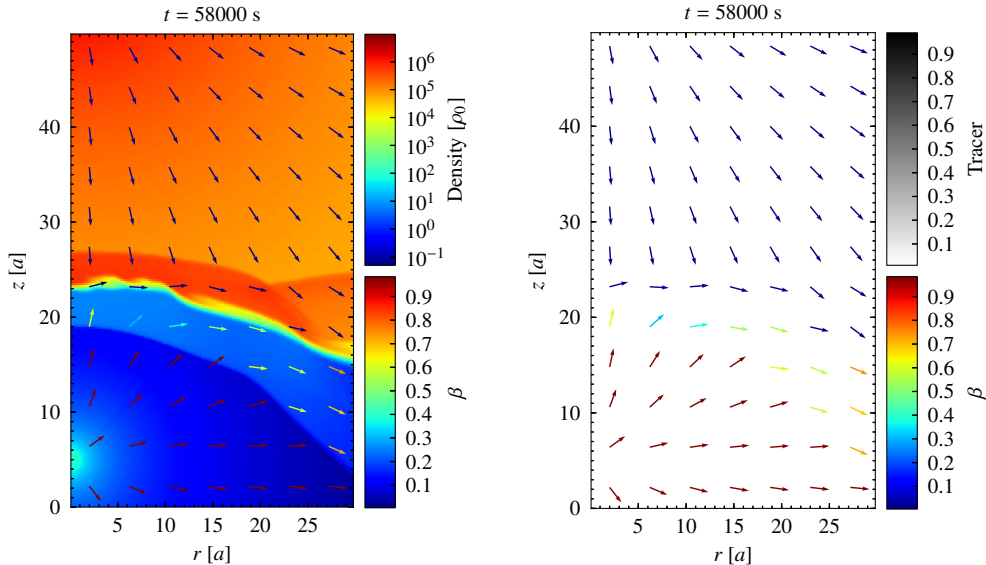
Results III — light and medium size clump



Clump: $\chi = 10$, $R_{\text{clump}} = 2.5 a = 2 \cdot 10^{11}$ cm

Code units: $\rho_0 = 22.5 \times 10^{-22}$ g cm $^{-3}$, $a = 8 \times 10^{10}$ cm | $d_{\text{star-pulsar}} = 4.4 \times 10^{12}$ cm.

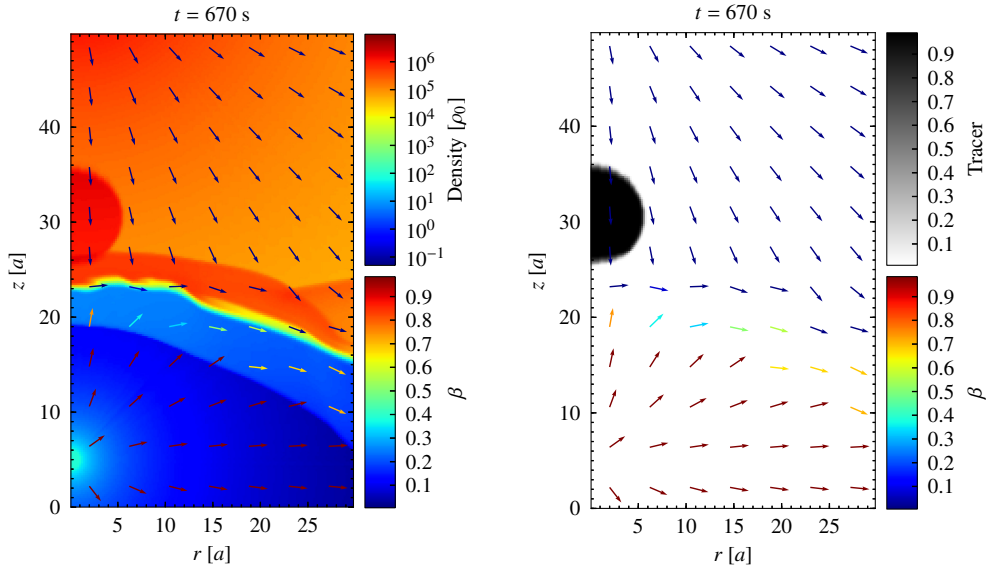
Results IV — light and large size clump



Clump: $\chi = 10$, $R_{\text{clump}} = 5 a = 4 \cdot 10^{11}$ cm

Code units: $\rho_0 = 22.5 \times 10^{-22}$ g cm $^{-3}$, $a = 8 \times 10^{10}$ cm | $d_{\text{star-pulsar}} = 4.4 \times 10^{12}$ cm.

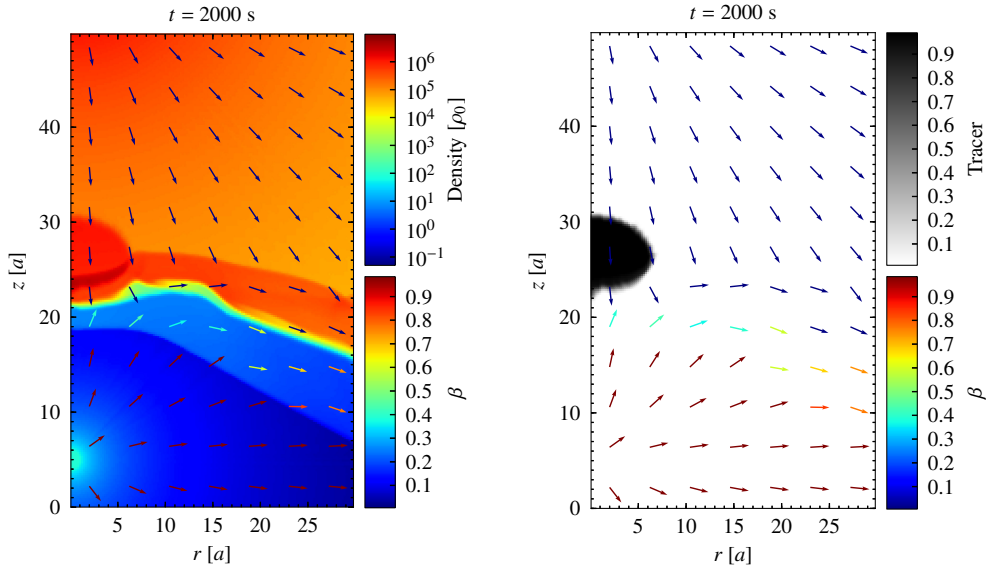
Results IV — light and large size clump



Clump: $\chi = 10$, $R_{\text{clump}} = 5 a = 4 \cdot 10^{11}$ cm

Code units: $\rho_0 = 22.5 \times 10^{-22}$ g cm $^{-3}$, $a = 8 \times 10^{10}$ cm | $d_{\text{star-pulsar}} = 4.4 \times 10^{12}$ cm.

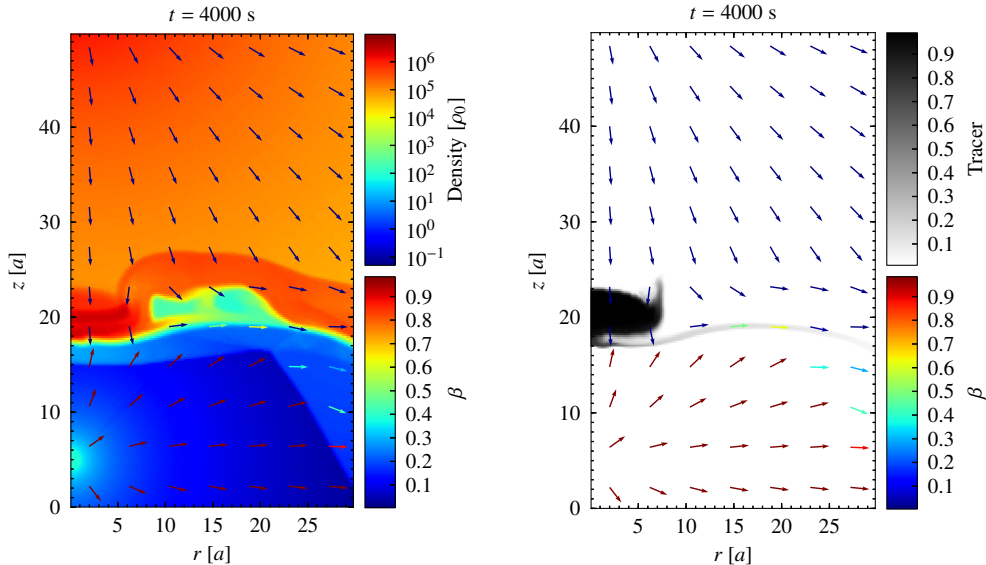
Results IV — light and large size clump



Clump: $\chi = 10$, $R_{\text{clump}} = 5 a = 4 \cdot 10^{11}$ cm

Code units: $\rho_0 = 22.5 \times 10^{-22}$ g cm $^{-3}$, $a = 8 \times 10^{10}$ cm | $d_{\text{star-pulsar}} = 4.4 \times 10^{12}$ cm.

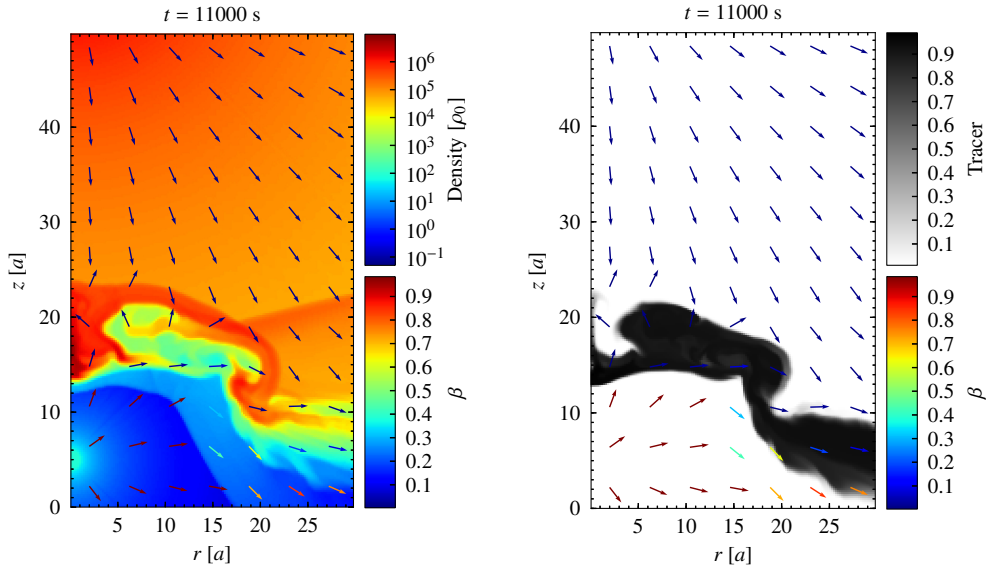
Results IV — light and large size clump



Clump: $\chi = 10$, $R_{\text{clump}} = 5 a = 4 \cdot 10^{11}$ cm

Code units: $\rho_0 = 22.5 \times 10^{-22}$ g cm $^{-3}$, $a = 8 \times 10^{10}$ cm | $d_{\text{star-pulsar}} = 4.4 \times 10^{12}$ cm.

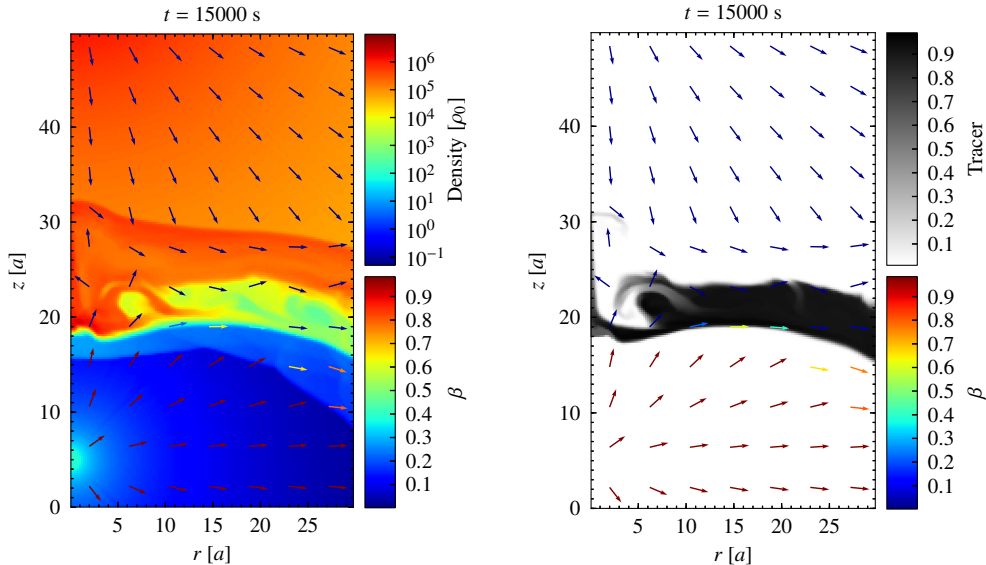
Results IV — light and large size clump



Clump: $\chi = 10$, $R_{\text{clump}} = 5 a = 4 \cdot 10^{11}$ cm

Code units: $\rho_0 = 22.5 \times 10^{-22}$ g cm⁻³, $a = 8 \times 10^{10}$ cm | $d_{\text{star-pulsar}} = 4.4 \times 10^{12}$ cm.

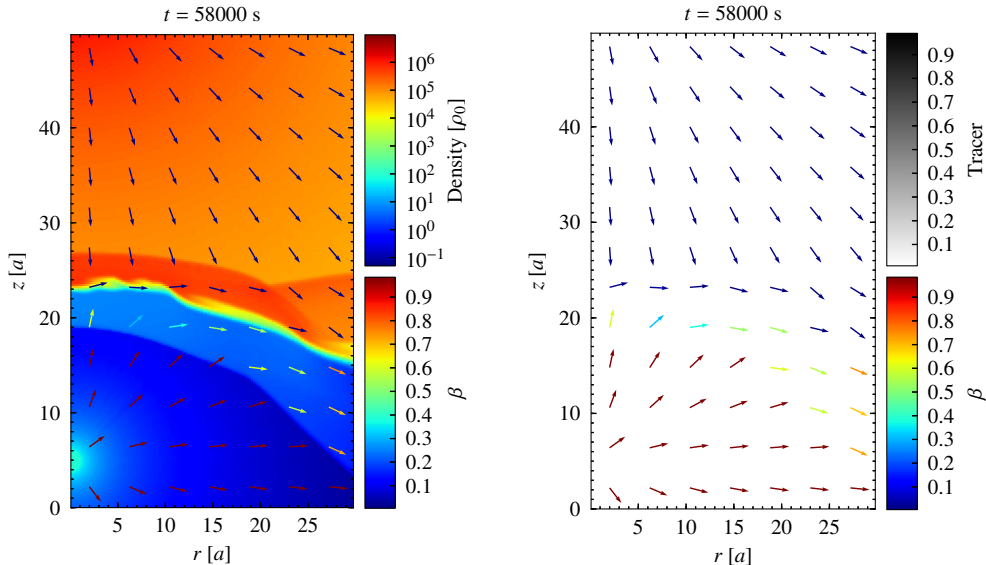
Results IV — light and large size clump



Clump: $\chi = 10$, $R_{\text{clump}} = 5 a = 4 \cdot 10^{11}$ cm

Code units: $\rho_0 = 22.5 \times 10^{-22}$ g cm $^{-3}$, $a = 8 \times 10^{10}$ cm | $d_{\text{star-pulsar}} = 4.4 \times 10^{12}$ cm.

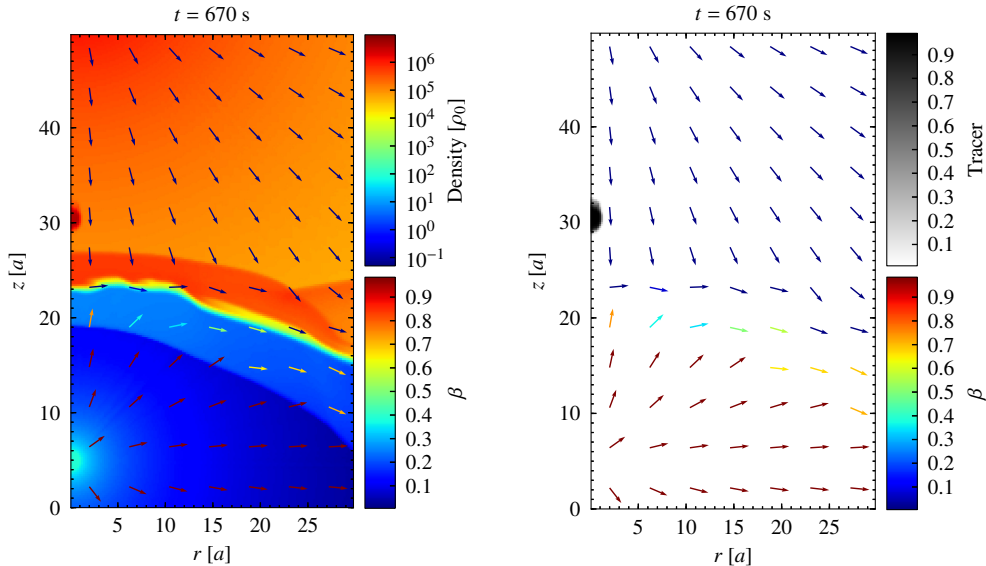
Results V — dense and small size clump



Clump: $\chi = 30$, $R_{\text{clump}} = 1.0 a = 8 \cdot 10^{10}$ cm

Code units: $\rho_0 = 22.5 \times 10^{-22}$ g cm $^{-3}$, $a = 8 \times 10^{10}$ cm | $d_{\text{star-pulsar}} = 4.4 \times 10^{12}$ cm.

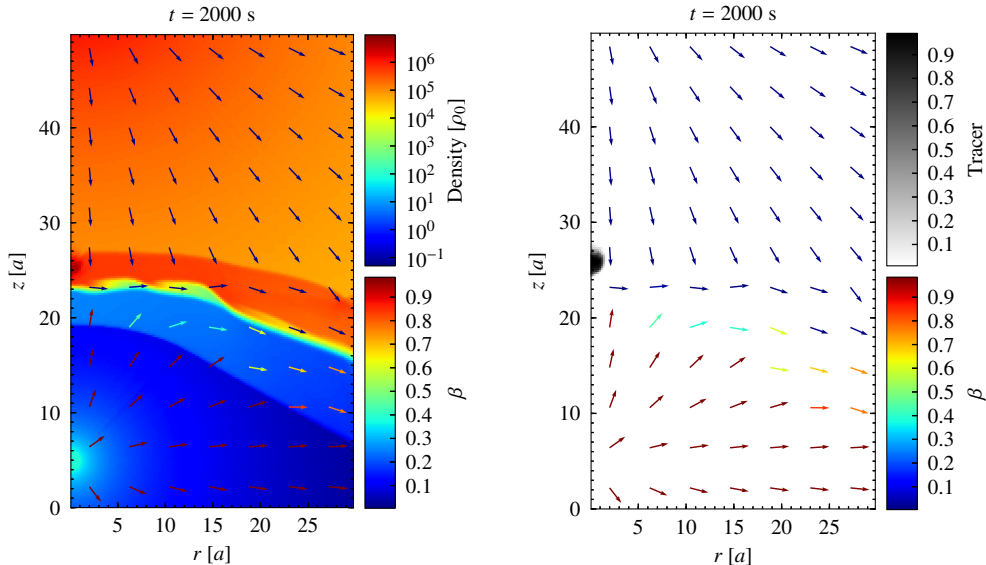
Results V — dense and small size clump



Clump: $\chi = 30$, $R_{\text{clump}} = 1.0 a = 8 \cdot 10^{10}$ cm

Code units: $\rho_0 = 22.5 \times 10^{-22}$ g cm $^{-3}$, $a = 8 \times 10^{10}$ cm | $d_{\text{star-pulsar}} = 4.4 \times 10^{12}$ cm.

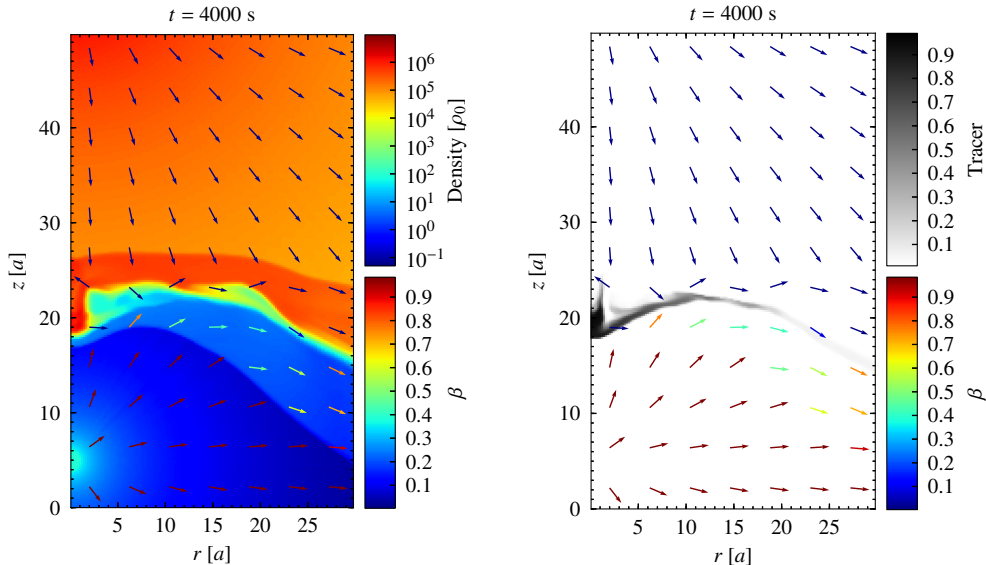
Results V — dense and small size clump



Clump: $\chi = 30$, $R_{\text{clump}} = 1.0 a = 8 \cdot 10^{10}$ cm

Code units: $\rho_0 = 22.5 \times 10^{-22}$ g cm $^{-3}$, $a = 8 \times 10^{10}$ cm | $d_{\text{star-pulsar}} = 4.4 \times 10^{12}$ cm.

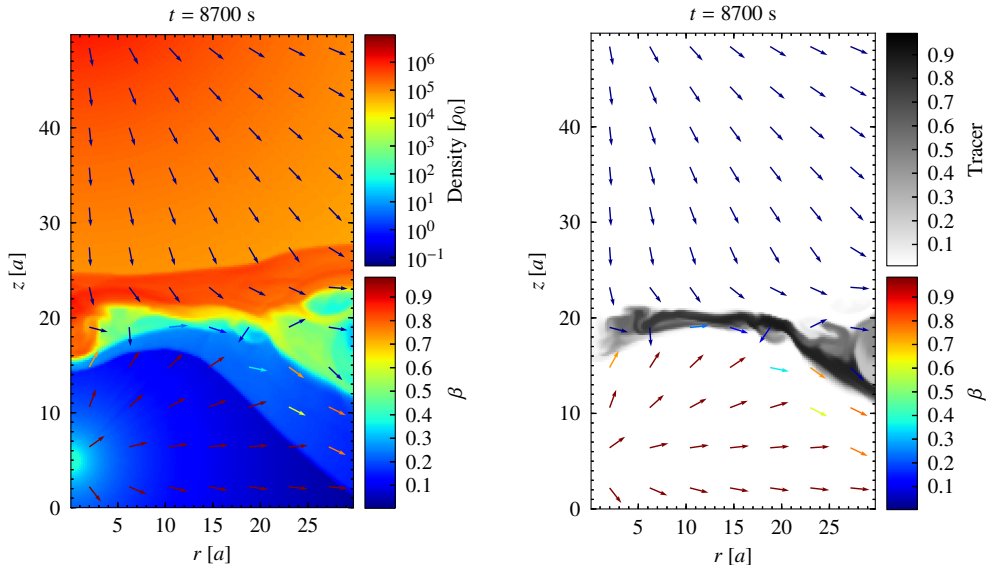
Results V — dense and small size clump



Clump: $\chi = 30$, $R_{\text{clump}} = 1.0 a = 8 \cdot 10^{10}$ cm

Code units: $\rho_0 = 22.5 \times 10^{-22}$ g cm $^{-3}$, $a = 8 \times 10^{10}$ cm | $d_{\text{star-pulsar}} = 4.4 \times 10^{12}$ cm.

Results V — dense and small size clump



Clump: $\chi = 30$, $R_{\text{clump}} = 1.0 a = 8 \cdot 10^{10}$ cm

Code units: $\rho_0 = 22.5 \times 10^{-22}$ g cm $^{-3}$, $a = 8 \times 10^{10}$ cm | $d_{\text{star-pulsar}} = 4.4 \times 10^{12}$ cm.

1. Introduction
2. Clump impact on the colliding wind region
3. Results
4. Discussion
5. Work in progress

General remarks:

- The **steady state** is very **sensitive** to the initial set-up parameters (grid size and density contrast / pulsar wind Lorentz Factor).
- The arrival of **clumps** can have very **strong impact** on the whole interaction structure (overcoming any possible numerical perturbation).
- The **clumps** trigger **Rayleigh-Taylor/Richtmyer-Meshkov and Kelvin-Helmholtz** instabilities leading to **quick changes** of the shocked pulsar-wind region (see also Bosch-Ramon et al. 2015).

Discussion II

Clump effects on the global structure and radiation:

- **Modest inhomogeneity degree:** non-negligible variations of the interaction structure and enhance the instability growth.
- **High inhomogeneity degree:** strong variations in the size of the two-wind interaction structure.
- **Both** generate quick and global variations in the **shocked pulsar wind**:
 - This affects the **location** of the pulsar wind **termination shock**, and therefore **reducing the emitter size** and increasing the magnetic field density (Bosch-Ramon 2013).
 - The relativistic **flow variations** on small spatial and temporal scales downstream of the pulsar wind shock **would lead to a complex radiative pattern in time and direction** caused by **Doppler boosting** (Khangulyan et al. 2014).

Discussion III

For the **PSR B1259–63 flare** observed by Fermi ~ 30 days after periastron passage (Abdo et al. 2011):

- The impact of a **piece of disk** on the two-wind interaction structure might have led to **efficient Compton scattering** by GeV electrons on local X-ray photons (Dubus & Cerutti 2013; Khangulyan et al. 2012 for IR photons), as a result of the strong **enhancement of the synchrotron photon density**.

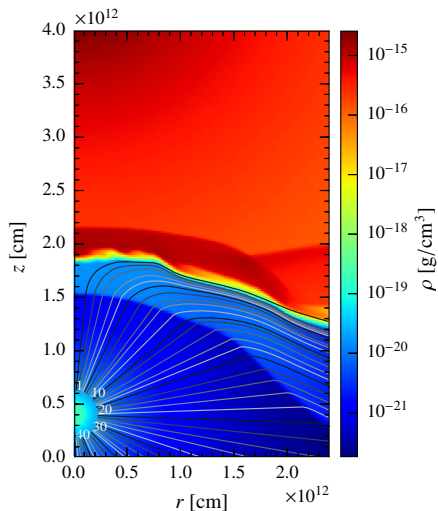
For the **short flares of scales** of second to hours found in **X-ray** lightcurves of **LS 5039 and LS I +61 303** (e.g., Bosch-Ramon et al. 2005; Paredes et al. 2007; Smith et al. 2009; Li et al. 2011):

- The impact of **clumps** might explain this short X-ray variability (Bosch-Ramon 2013).

Outline

1. Introduction
2. Clump impact on the colliding wind region
3. Results
4. Discussion
5. Work in progress

Work in progress — Radiative output



- V.M. de la Cita, V. Bosch-Ramon, X. Paredes-Fortuny, D. Khangulyan, M. Perucho, and M. Ribó in **prep.**
- **Tomorrow's talk by Moreno de la Cita, Víctor at 9:50** on the same radiative code but applied to star-jet interactions in AGN.

Backup slides

Backup slides

Stellar and pulsar parameters

Table 1: Wind velocity v , specific internal energy ϵ , and density ρ at a distance $r = 8 \times 10^{10}$ cm with respect to the star and pulsar centres located at (r_0, z_0) .

Parameter	Stellar wind	Pulsar wind
v	$3 \times 10^8 \text{ cm s}^{-1}$	$2.94 \times 10^{10} \text{ cm s}^{-1}$
ϵ	$1.8 \times 10^{15} \text{ erg g}^{-1}$	$9 \times 10^{19} \text{ erg g}^{-1}$
ρ	$2.68 \times 10^{-13} \text{ g cm}^{-3}$	$1.99 \times 10^{-19} \text{ g cm}^{-3}$
(r_0, z_0)	$(0, 4.8 \times 10^{12} \text{ cm})$	$(0, 4 \times 10^{11} \text{ cm})$

- Typical physical values in gamma-ray binaries:

$$R_* \sim 10 R_\odot,$$

$$d_{\text{star-pulsar}} \sim 10^{13} \text{ cm},$$

$$R_{\text{clump}} \approx 0.2 d_{\text{star-pulsar}}$$

High resolution simulations

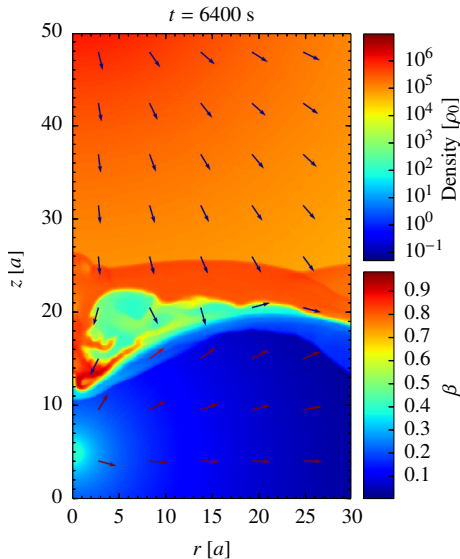


Figure 1: Resolution 1.5 times higher. Clump: $\chi = 10$, $R_{\text{clump}} = 2.5 a = 2 \cdot 10^{11}$ cm.

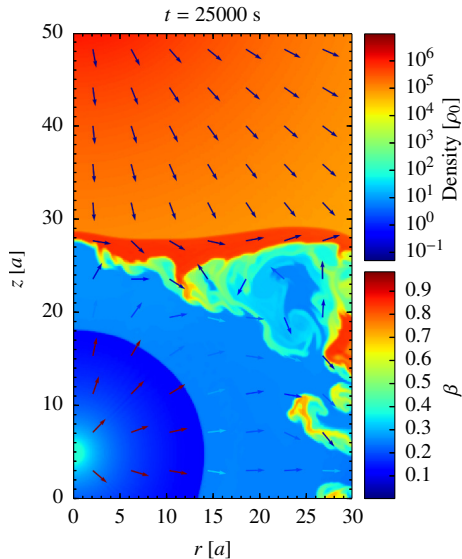
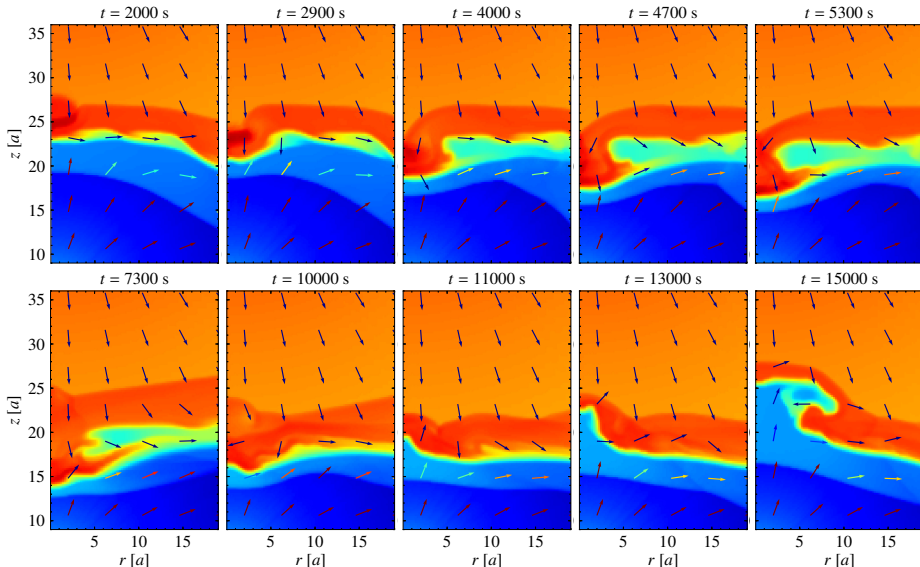


Figure 2: Resolution 2 times higher. Steady state not reached.

Results — light and medium size clump



Clump: $\chi = 10$, $R_{\text{clump}} = 2.5 a = 2 \cdot 10^{11}$ cm

Code units: $\rho_0 = 22.5 \times 10^{-22}$ g cm $^{-3}$, $a = 8 \times 10^{10}$ cm | $d_{\text{star-pulsar}} = 4.4 \times 10^{12}$ cm.